Analysis of Optimal Cost-Effectiveness in the COVID-19 Epidemic Model by Considering Quarantine, Hospitalization, and the Environment

Marsudi, Nur Shofianah, and Ummu Habibah, *Member IAENG*

***Abstract*—In this paper, the population dynamics of a novel coronavirus are studied. An extended SEIR model with quarantine, hospitalization, and the environment compartment is proposed to simulate the novel coronavirus epidemic. The model considers eight distinct epidemiological classes: susceptible, exposed, asymptomatic, symptomatic, quarantined, hospitalized, recovered, and viruses in the environment. The basic reproduction numbers are determined by using a method called the next-generation matrix. The model has two equilibria: a disease-free equilibrium and an endemic equilibrium. The Lyapunov function and the LaSalle invariance principle are used to analyze the global asymptotical stability of the equilibria of the proposed model. The disease-free equilibrium is globally asymptotically stable if the basic reproduction number is less than unity, and the endemic equilibrium is globally asymptotically stable if the basic reproduction number is greater than unity. To study cost-effectiveness assessments for the four optimum control strategies, we ran numerical simulations. When the four control strategies were compared, it was discovered that Strategy A (public health education and intensive medical treatment) was the most economical and efficient control intervention in the absence of vaccination. However, we observe that strategies A, B, and D are similarly effective at containing COVID-19 in terms of infection prevention.**

***Index Terms*—COVID-19 model, global stability, quarantine, hospitalization, optimal control.**

I. Introduction

THE World Health Organization (WHO) designated the novel coronavirus (COVID-19) as a public health emergency of international concern (PHEIC) on January 30, 2020.On February 12, 2020, a brand-new coronavirus disease in humans was given the name "Coronavirus Disease" by the World Health Organization. In March 2020, WHO proclaimed COVID-19 a global pandemic [1]. The spread of the COVID-19 virus can occur due to direct or indirect physical contact with the sufferer. Indirect transmission can occur when viruses in patient droplets are inhaled by humans [2]. The virus can survive for up to three days on plastic and stainless steel, or it can survive in aerosols for up to three hours [3]. The spread of COVID-19 is difficult to detect because it can be transmitted by people without symptoms. The outbreak and spread of COVID-19 have prompted governments and health authorities in various countries to take the necessary actions to stop the spread of COVID-19. Pharmaceutical or non-medical interventions that can be carried out by all parties under the coordination of the local government, for example, public health education campaigns, implementing clean and healthy behavior through health protocols (washing hands with soap, wearing a mask, not smoking, consuming balanced nutrition, staying at home, avoiding crowds, keeping the environment clean, etc.), and ensuring the availability of support (PCR tests). The growth of the COVID-19 epidemic is extremely serious and constitutes a significant threat to public health security and the global economy, so COVID-19 must be controlled.

Until now, the mechanism of the spread of COVID-19 has been studied for prevention and control purposes. One approach to understanding the dynamics of the spread of infectious diseases is through mathematical modelling. Mathematical models can help us understand the transmission and control mechanisms of new infectious diseases like COVID-19. In the absence of vaccines or pharmaceutical interventions, mathematical modelling can be used to evaluate non-medical preventative strategies or non-pharmaceutical interventions ([4]-[8]). Many new epidemic model are based on the classic SEIR (Susceptible-Exposed-Infectious-Recovered). Several COVID-19 epidemic models based on the classic SEIR compartment model are now being utilized to simulate COVID-19 disease dynamics ([9]-[12]). Zhao *et al*. [13] investigated an adapted SEIR model to forecast COVID-19 spread in South Africa, Egypt, Algeria, Nigeria, Senegal, and Kenya. Similarly, [14] investigated the expansion of the SEIR model using model parameters derived from epidemiological data and estimates based on data from West Java Province, Indonesia. Obsu and Balcha [15] used a COVID-19 mathematical model that included three time-dependent control functions: preventive control measures (quarantine, isolation, and social distancing), disinfection of contaminated surfaces, and

Manuscript received July 03, 2023; revised October 11, 2023.

This work is supported by the FMIPA DLK research grand scheme of Universitas Brawijaya with contract No. 3110.2/UN10.F09/PN/2022.

Marsudi is an Associate Professor in the Department of Mathematics, Universitas Brawijaya, Malang, Indonesia (corresponding author to provide e-mail: marsudi61@ub.ac.id).

Nur Shofianah is a Lecturer in the Department of Mathematics, Universitas Brawijaya, Malang, Indonesia (e-mail: nur_shofianah @ub.ac.id)

Ummu Habibah is a Lecturer in the Department of Mathematics Universitas Brawijaya, Malang, Indonesia (e-mail: ummu_habibah @ub.ac.id).

infected individuals at home. Rapid testing, medical masks, increased medical care in hospitals, and public awareness are among the interventions investigated by the authors. Furthermore, [16] conducted a mathematical study on the spread of COVID-19 while taking social distancing and rapid assessment into account in the case of Jakarta, Indonesia. Luo *et al*. [17] studied the contribution of non-pharmaceutical interventions to the control of COVID-19 in China based on a pairwise model. Asamoah et al. [18] use data from Ghana to investigate the global stability and cost-effectiveness of COVID-19 in terms of environmental impact. They then used cost-effectiveness analysis to look at optimal control and economic outcomes. Following that, Asamoah *et al*. [19] look into the sensitivity and an economic evaluation of a new model to study the COVID-19 epidemic and its control measures to find the best solution. Their main discovery was that it is better to have two ways to control a situation (reducing transmission and isolating cases) instead of just one way, even though it may be more expensive.

According to the facts and descriptions above, COVID-19 is currently a health problem in all countries. If vaccine availability is limited, public health education campaign interventions, quarantine, self-isolation, early diagnosis and treatment, and surface disinfection are the top priority programs for preventing the spread of COVID-19. This is where the significance of this study lies: examining the impact of nonpharmaceutical and medical interventions using mathematical models. In this study, the model framework refers to the model from [18], which was expanded by adding quarantine and hospital compartments.

The aim of this research is to analyze optimal control and Analyzing the best way to control the transmission of COVID-2019 and the cost-effectiveness of implementing public health education (awareness the medical mask, stay at home, and washing their hands), intense medical treatment, and surface disinfection. It is recommended to use a bigger SEIR model: Susceptible, Exposed, Asymptomatic Infectious, Symptomatic Iinfectious, Quarantined, Hospitalized, and Recovered.

The organization of this paper is as follows: In the next section, the epidemic model, positivity, and boundedness of the solutions are shown in Section 2. In Section 3, the model analysis is discussed, comprising the equilibrium point, the basic reproduction number, and an examination of the global stability of the equilibrium point. The sensitivity analysis of the basic reproduction number is presented in Section 4. Section 5 defines the optimal control problem, characterizes the optimal control, and presents numerical simulations. Section 6 contains the cost-effectiveness analysis. In Section 7, several conclusions are offered as a conclusion.

II. Model Formulation

We assumed that the total population is divided into eight distinct epidemiological classes: susceptible class or individuals who are susceptible to the COVID-19 virus ($S(t)$), exposed class or individuals who have been infected, but are not infectious ($E(t)$), asymptomatic class or individuals who are infectious yet do not exhibit symptoms ($A(t)$), symptomatic class or someone who has COVID-19 symptoms and can transfer the illness ($I(t)$), quarantined asymptomatic class or individuals with infectious diseases yet show no symptoms are quarantined ($Q(t)$), hospitalized or isolated symptoms class or individuals with infectious diseases who are admitted to a medical facility ($H(t)$), recovered class or those who have recovered from the illness ($R(t)$), and the concentration of the SARS-CoV-2 in the environment ($B(t)$). The total population of humans at time t is $N(t) = S(t) + E(t) + A(t) + I(t) + Q(t) + H(t) + R(t)$. A flow diagram of each compartment's dynamics in model (1) is shown in Fig. 1.

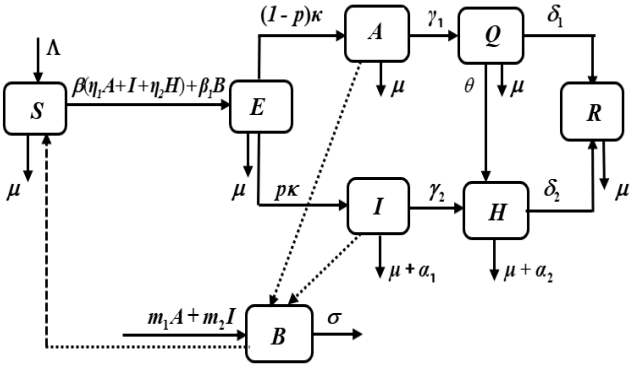

Fig. 1. Schematic diagram of the deterministic model (1).

The corresponding systems of differential equations and the description of the parameters are, respectively, given in (1) and Table I.

$$\begin{aligned}
\frac{dS}{dt} &= \Lambda - [\beta(\eta_1 A + I + \eta_2 H) + \beta_1 B]S - \mu S,\\
\frac{dE}{dt} &= [\beta(\eta_1 A + I + \eta_2 H) + \beta_1 B]S - (\kappa + \mu)E,\\
\frac{dA}{dt} &= (1-p)\kappa E - (\gamma_1 + \mu)A,\\
\frac{dI}{dt} &= p\kappa E - (\gamma_2 + \alpha_1 + \mu)I\\
\frac{dQ}{dt} &= \gamma_1 A - (\theta + \delta_1 + \mu)Q,\\
\frac{dH}{dt} &= \gamma_2 I + \theta Q - (\delta_2 + \alpha_2 + \mu)H,\\
\frac{dR}{dt} &= \delta_1 Q + \delta_2 H - \mu R,\\
\frac{dB}{dt} &= m_1 A + m_2 I - \sigma B.
\end{aligned} \tag{1}$$

The non-negative initial conditions of the system of model (1) are denoted by $S(0) > 0, E(0) \geq 0, A(0) \geq 0, I(0) \geq 0, Q(0) \geq 0, H(0) \geq 0, R(0) \geq 0, B(0) \geq 0.$

We simplify the equation of system (1) to get the total differential equation as

$$\begin{aligned}
\frac{dN}{dt} &= \Lambda - \mu N - \alpha_1 I - \alpha_2 H,\\
\frac{dB}{dt} &= m_1 A + m_2 I - \alpha B.
\end{aligned} \tag{2}$$

The model developed assumed that susceptible individuals are continuously recruited (by birth or immigration) into the population at a constant rate Λ. The susceptible individuals acquire the COVID-19 infection when they interact with the infected individuals in $A, I, H,$ and B compartments. According to the assumption that the frequency of human-pathogen interactions is bilinear with the intensity of infection, $\lambda = \beta(\eta_1 A + I + \eta_2 H) + \beta_1 B,$ where the parameter β shows the effective contact rates from asymptomatic, symptomatic, and hospitalized classes and β_1 shows the effective contact rates of the virus in the environment class. The parameter η_1 $(0 \le \eta_1 \le 1)$ accounts for the expected reduction in disease transmissibility of asymptomatic infected individuals versus symptomatic infected individuals. The parameter η_2 is used for the infectiousness rate among COVID-19 hospitalized patients. Following the completion of the incubation period, the latent individuals develop an infection and become infected at the rate κ and proportion denoted by p enters the symptomatic infected class after exhibiting disease symptoms, while the remainder with no symptoms join the asymptomatic infected compartment. Asymptomatic individuals who have contact with COVID-19-infected patients are discovered (by contact-tracing) and placed in quarantine at a rate of γ_1, progression rate from quarantined to the hospitalized class at a rate θ. Symptomatic infected individuals have been confirmed (after testing) and placed in hospitals at a rate of γ_2. The parameters δ_1 and δ_2 represent the recovery rates of quarantined and hospitalized classes, respectively. Last but not least, α_1 and α_2 indicate, respectively, the COVID-19-induced death rate for people in the I and H classes. The natural death rate in all classes is denoted by μ. Here every state variables and parameters are considered to be positive for every $t > 0$.

In order for the system (1) to be biologically valid, the model's solution must be both positive and bounded for every time $t > 0$. The following lemmas provide the proof:

Lemma 1. *If* $D(t) = (S(t), E(t), A(t), I(t), Q(t), H(t), R(t), B(t))$ *with the initial condition, then the solution* $D(t)$ *of system (1)* is *nonnegative for every* $t > 0$. *Also,* $\limsup_{t\to\infty} N(t) = \Lambda / \mu$ *and* $\limsup_{t\to\infty} B(t) = \Lambda(m_1 + m_2) / \sigma\mu$.

Proof. Let $t_1 = \sup\{t > 0 : D(t) > 0 \text{ in } [0, t]\}$. Thus, $t_1 > 0$. From the first equation of the system (1), we have

$$\frac{dS}{dt} = \Lambda - (\lambda + \mu)S, \tag{3}$$

With $\lambda = \beta(\eta_1 A + I + \eta_2 H) + \beta_1 B$. Using the integrating factor and the technique of variable separation, (3) can be expressed as

$$\frac{dS}{dt}\left[S(t)\exp\{\mu v + \lambda(v)dv\}\right] = \Lambda \exp\{\mu v + \lambda(v)dv\}. \tag{4}$$

TABLE I
DESCRIPTION OF THE PARAMETERS OF THE MODEL (1)

Parameter	Description
Λ	The recruitment rate of susceptible
β	Effective contact rates from asymptomatic, symptomatic and hospitalized classes
β_1	Effective contact rate from the environment
μ	Natural death rate
η_1	Relative transmissibility of asymptomatic class
η_2	Relative transmissibility of hospitalized class
p	The proportion of individuals who receive a timely diagnosed
κ	The probability of exposed people becoming infected
γ_1	The quarantined rate
γ_2	The hospitalized rate
α_1	The disease-induced death rate at I_2 class
α_2	The disease-induced death rate at H class
δ_1	Recovery from quarantined class
δ_2	Recovery from hospitalized class
σ	The natural decay rate of virus from the environment (surfaces)
θ	Progression rate from quarantined to the hospitalized
m_1	Virus contribution due to I_1 into the environment
m_2	Virus contribution due to I_2 into the environment

Integrating (4) in the range [0, t_1] we get,

$$S(t_1)\exp\left\{\mu t_1 + \int_0^{t_1}\lambda(u)\,du\right\} - S(0) = \int_0^{t_1}\Lambda\exp\left\{\mu x + \int_0^{x}\lambda(v)\,dv\right\}dx.$$

So,

$$S(t_1) = \left[S(0) + \int_0^{t_1}\Lambda\exp\{\mu x + \lambda(v)dv\}\,dx\right]\exp\left\{-\left(\mu t_1 + \int_0^{t_1}\lambda(u)du\right)\right\} > 0. \tag{5}$$

For the remaining equations, we follow the same procedures as in the equation for system (1) above to show $D(t) > 0$ for all $t > 0$. As a result, the first portion of the lemma is established.

As for the second portion of the lemma, it should be emphasized that

$$0 < S(t), E(t), A(t), I(t), Q(t), H(t), R(t) \le N(t) \le \frac{\Lambda}{\mu},$$
$$0 < B(t) \le \frac{\Lambda(m_1 + m_2)}{\mu\sigma}.$$

If the first seven equations of system (1) are added, we get

$$\frac{dN}{dt} = \Lambda - \mu N - (\alpha_1 I + \alpha_2 H) \le \Lambda - \mu N. \tag{6}$$

From the last equation of system (1), we have

$$\frac{dB}{dt} = m_1 A + m_2 I - \sigma B. \tag{7}$$

When we combine and subtract limsup and liminf for $t \to \infty$ in (6) and (7), we get

$$\Lambda / \mu \le \liminf_{t\to\infty} N(t) \le \limsup_{t\to\infty} N(t) \le \Lambda / \mu$$

and

$$\Lambda(m_1 + m_2) / \sigma\mu \le \liminf_{t\to\infty} B(t) \le \limsup_{t\to\infty} B(t) \le \Lambda(m_1 + m_2) / \sigma\mu.$$

Thus, $\limsup_{t\to\infty} N(t) = \Lambda/\mu$ and $\limsup_{t\to\infty} B(t) = \Lambda(m_1+m_2)/\sigma\mu$.

The proof of Lemma 2 is completed. □

The closed region will be defined as a positively invariant set in the following lemma. Using our COVID-19 model, the area shown below will be analyzed. Consider the area that is feasible

$$\Omega = \Omega_h \times \Omega_b \subset \mathbb{R}_+^4 \times \mathbb{R}_+,$$

where

$$\Omega_h = \{(S,E,A,I,Q,H,R) \in \mathbb{R}_+^7 : N \le \Lambda/\mu\}$$

and

$$\Omega_b = \{B \in \mathbb{R}_+ : B \le \Lambda(m_1+m_2)/\mu\sigma\}.$$

Lemma 2. *The closed region* $\Omega \subset \mathbb{R}_+^8$ *given below is a positively invariant set with a non-negative initial condition for the system* (*1*) *in* $\mathbb{R}_+^8$.

$$\Omega = \{(S,E,A,I,Q,H,R,B) \in \mathbb{R}_+^8 : N \le \Lambda/\mu,\ B \le \Lambda(m_1+m_2)/\mu\sigma\}. \quad (8)$$

Proof. From (6) and (7), we have

$$\frac{dN(t)}{dt} \le \Lambda - \mu N \quad \text{and} \quad \frac{dB(t)}{dt} \le \frac{\Lambda m}{\mu} - \sigma B,$$

where $m = m_1 + m_2$.

Integrating both sides of the above two inequality equations and applying the comparison [20] when $t \to \infty$, we obtain

$$N(t) \le N(0)e^{-\mu t} + \frac{\Lambda}{\mu}\left(1 - e^{-\mu t}\right) = \frac{\Lambda}{\mu} + \left(N(0) - \frac{\Lambda}{\mu}\right)e^{-\mu t}$$

and

$$B(t) \le \frac{m\Lambda}{\sigma\mu} + \left(B(0) - \frac{m\Lambda}{\sigma\mu}\right)e^{-\alpha t}.$$

Clearly, $0 < N(t) \le \Lambda/\mu$ and $0 < B(t) \le m\Lambda/\sigma\mu$, as $t \to \infty$. In particular, $N(t) \le \Lambda/\mu$ if $N(0) \le \Lambda/\mu$ and $B(t) \le m\Lambda/\sigma\mu$ if $B(0) \le m\Lambda/\sigma\mu$. Thus, the region Ω is positive invariant and attracts all possible solutions of the system (1). Thus, $S(t), E(t), A(t), I(t), Q(t), H(t), R(t)$, and $B(t)$ are bounded.

The proof of Lemma 2 is completed. □

III. Model Analysis

We will perform a qualitative analysis of the system (1) in this part.

A. The Equilibrium Points

In this section, the equilibrium points of system (1) will be calculated. For convenience, we note $k_1 = \kappa + \mu$, $k_2 = \gamma_1 + \mu$, $k_3 = \gamma_2 + \alpha_1 + \mu$, $k_4 = \theta + \delta_1 + \mu$, and $k_5 = \delta_2 + \alpha_2 + \mu$.

The equilibrium points of system (1) is obtained by solving the following system

$$\begin{aligned}
\Lambda - [\beta(\eta_1 A + I + \eta_2 H) + \beta_1 B]S - \mu S &= 0\\
[\beta(\eta_1 A + I + \eta_2 H) + \beta_1 B]S - k_1 E &= 0\\
(1-p)\kappa E - k_2 A &= 0\\
p\kappa E - k_3 I &= 0\\
\gamma_1 A - k_4 Q &= 0\\
\gamma_2 I + \theta Q - k_5 H &= 0\\
\delta_1 Q + \delta_2 H - \mu R &= 0\\
m_1 A + m_2 I - \sigma B &= 0.
\end{aligned} \quad (9)$$

From the system (9) and some algebraic manipulations, we have

$$\begin{aligned}
A &= \frac{(1-p)\kappa E}{k_2},\ I = \frac{p\kappa E}{k_3},\ Q = \frac{\gamma_1(1-p)\kappa E}{k_2 k_4},\\
H &= \frac{(bd\gamma_2 p\kappa + c\gamma_1(1-p)\kappa)E}{k_2 k_3 k_4 k_5},\\
R &= \frac{\delta_1\gamma_1(1-p)\kappa E}{\mu bd} + \frac{\delta_2(k_2 k_4\gamma_2 p\kappa + c\gamma_1(1-p)\kappa)E}{\mu k_2 k_3 k_4 k_5},\\
B &= \frac{[k_3 m_1 p\kappa + k_2 m_2(1-p)\kappa]E}{k_2 k_3 \sigma}.
\end{aligned} \quad (10)$$

Substituting (10) in the second equation of system (1) gives

$$\left\{\left[\frac{\beta\kappa\{\eta_1 k_3 k_4 k_5(1-p) + \eta_2\gamma_1 k_3\theta(1-p) + \eta_2\gamma_2 k_3 k_4 p + k_2 k_4 k_5 p\}}{k_2 k_3 k_4 k_5} - \frac{\beta_1\kappa[k_3 m_1(1-p) + k_2 m_2 p]}{k_2 k_3 \sigma}\right]S - k_1\right\}E = 0. \quad (11)$$

B. Disease-Free Equilibrium and Basic Reproduction Number

The first case in (11) if $E = 0$, results in the disease-free equilibrium point, given by

$$X_0 = \left(\frac{\Lambda}{\mu}, 0, 0, 0, 0, 0, 0\right). \quad (12)$$

The expected value of the infection rate per time unit is the basic reproduction number, denoted as $\mathcal{R}_0$. An infected person is the source of the infection, which affects a susceptible population. In the following, we will find that the basic reproduction number $\mathcal{R}_0$ of system (1) is computed using the next-generation matrix method formulated in [21].

Let $X = (E, A, I, Q, H, B)^T$, $k_1 = \kappa + \mu$, $k_2 = \gamma_1 + \mu$, $k_3 = \gamma_2 + \alpha_1 + \mu$, $k_4 = \theta + \theta_1 + \mu$, and $k_5 = \delta_2 + \alpha_2 + \mu$. Without loss of generality, system (1) can be written as

$$\frac{dX}{dt} = \mathcal{F}(X) - \mathcal{V}(X) \quad (13)$$

where

$$\mathcal{F}(X)=\begin{pmatrix}\beta(\eta_1 A+I+\eta_2 H)S+\beta_1 BS\\0\\0\\0\\0\\0\end{pmatrix},\ \mathcal{V}(X)=\begin{pmatrix}k_1E\\-(1-p)\kappa E+k_2A\\-p\kappa E+k_3I\\-\gamma_1 A+k_4Q\\-\gamma_2 I-\theta Q+k_5H\\-m_1A-m_2I+\sigma B\end{pmatrix}. \tag{14}$$

By calculating, we obtain the Jacobian matrices of $\mathcal{F}(X)$ and $\mathcal{V}(X)$ at the disease-free equilibrium X_0 are respectively,

$$F=\begin{pmatrix}0&\frac{\beta\eta_1\Lambda}{\mu}&\frac{\beta\Lambda}{\mu}&0&\frac{\beta\eta_2\Lambda}{\mu}&\frac{\beta_1\Lambda}{\mu}\\0&0&0&0&0&0\\0&0&0&0&0&0\\0&0&0&0&0&0\\0&0&0&0&0&0\\0&0&0&0&0&0\end{pmatrix},V=\begin{pmatrix}k_1&0&0&0&0&0\\-(1-p)\kappa&k_2&0&0&0&0\\-p\kappa&0&k_3&-\theta&0&0\\0&-\gamma_1&0&k_4&0&0\\0&0&-\gamma_2&-\theta&k_5&0\\0&-m_1&-m_2&0&0&\sigma\end{pmatrix}. \tag{15}$$

Now, FV^{-1} is the generation matrix of system (1) and the basic reproduction number of system (1) is obtained as the spectral radius $\rho(FV^{-1})$ that is the dominant eigen value of the matrix FV^{-1}, denoted by $\mathcal{R}_0$, is thus given by

$$\begin{aligned}\mathcal{R}_0&=\frac{\beta\eta_1\Lambda\kappa(1-p)}{\mu k_1k_2}+\frac{\beta\Lambda\kappa p}{\mu k_1k_3}+\frac{\beta\eta_2\Lambda\kappa[\gamma_1k_3\theta(1-p)+\gamma_2k_2k_4p]}{\mu k_1k_2k_3k_4k_5}\\&\quad+\frac{\beta_1\Lambda\kappa[k_3m_1(1-p)+k_2m_2p]}{\mu k_1k_2k_3\sigma}\\&=\mathcal{R}_{0A}+\mathcal{R}_{0I}+\mathcal{R}_{0H}+\mathcal{R}_{0B}\end{aligned} \tag{16}$$

where $\mathcal{R}_{0A},\mathcal{R}_{0I},\mathcal{R}_{0H}$, and $\mathcal{R}_{0B}$ are the proportions of the basic reproduction number contributed by the asymptomatic infected class, the symptomatic infected class, the hospitalized infected class, and the virus in the environment class, respectively. The basic reproduction number represents the number of new infected individuals caused by a primary infected individual during the infection period in totally susceptible individuals.

C. Endemic Equilibrium

Let us suppose that $X_1=(S^*,E^*,A^*,I^*,Q^*,H^*,R^*,B^*)$ represents an endemic equilibrium of system (1). The second case in (11) if $E\neq 0$ implies that

$$S^*=\frac{\Lambda}{\mu\mathcal{R}_0}. \tag{17}$$

By adding the first two equations of system (9), we substitute S^* from (17) and simplify E^* we get

$$E^*=\frac{\Lambda-\mu S^*}{k_1}=\frac{\Lambda}{k_1}\left(\frac{\mathcal{R}_0-1}{\mathcal{R}_0}\right). \tag{18}$$

Hence, $E^*>0$ whenever $\mathcal{R}_0>0$. Thus, the other components of the endemic equilibrium X_1 can then be obtained by substituting the unique value of E^* give in (18) into the steady-state expressions in (10), we obtain

$$\begin{aligned}&A^*=\frac{(1-p)\kappa E^*}{k_2},\ I^*=\frac{p\kappa E^*}{k_3},\ Q^*=\frac{\gamma_1(1-p)\kappa E^*}{k_2k_4},\\&H^*=\frac{(bd\gamma_2p\kappa+c\gamma_1(1-p)\kappa)E^*}{k_2k_3k_4k_5},\\&R^*=\frac{\delta_1\gamma_1(1-p)\kappa E^*}{\mu bd}+\frac{\delta_2[k_2k_4\gamma_2p\kappa+c\gamma_1(1-p)\kappa]E^*}{\mu k_2k_3k_4k_5},\\&B^*=\frac{[k_3m_1p\kappa+k_2m_2(1-p)\kappa]E^*}{k_2k_3\sigma}.\end{aligned} \tag{19}$$

D. Global Stability of the Disease-free Equilibrium

We shall demonstrate the global stability of the disease-free equilibrium X_0 in this subsection to confirm that the COVID-19 disease has been eradicated. For this purpose, we consider the feasible region

$$\Omega_1=\left\{(S,E,A,I,Q,H,R,B)\in\Omega: S\le S^0\right\}.$$

Lemma 3. *For the system (1), the region Ω_1 is positively invariant.*

Proof. From the first equation of system (1), we have

$$\begin{aligned}\frac{dS}{dt}&=\Lambda-[\beta(\eta_1A+I+\eta_2H)+\beta_1B]S-\mu S\\&\le\Lambda-\mu S=\mu\left(\frac{\Lambda}{\mu}-S\right)\\&=\mu\left(S^0-S\right)\text{ as }S^0=\Lambda/\mu.\end{aligned} \tag{20}$$

In order to solve the differential equations (20), we use the comparison theorem [33],

$$S(t)\le S^0-\left(S^0-S(0)\right)e^{-\mu t}.$$

So, if $S(0)\le S^0$ is true for all $t\ge 0$, then $S(t)\le S^0$ is true for all $t\ge 0$. Hence, we have the region Ω_1 is positively invariant and attracts all solutions of system (1).

The proof of Lemma 3 is completed. □

The global asymptotic stability for the disease-free equilibrium of system (1) will be examined in the following theorem. We applied the approach suggested by [22] to look into the global stability of X_0.

Theorem 1. *If $\mathcal{R}_0\le 1$, then the disease-free equilibrium X_0 of system (1) is globally asymptotically stable in Ω.*

Proof. Let $Y_1=(S,R)\in\mathbb{R}^2$ represents the uninfected compartments, $Y_2=(E,A,I,Q,H,B)\in\mathbb{R}^6$ represents the infected compartments, and the disease-free equilibrium of system (1), $X_0=(\Lambda/\mu,0,0,0,0,0,0,0)=(Y_1^0,0,0,0,0,0,0,0)$ where $Y_1^0=(S^0,R^0)=(\Lambda/\mu,0)$. System (1) can be written as

$$\begin{aligned}&\frac{dY_1}{dt}=F(Y_1,0),\\&\frac{dY_2}{dt}=G(Y_1,Y_2),\ G(Y_1,0)=0,\end{aligned}\tag{21}$$

where

$$F(Y_1,Y_2)=\begin{pmatrix}\Lambda-[\beta(\eta_1A+I+\eta_2H)+\beta_1B]S-\mu S\\ \delta_1Q+\delta_2H-\mu R\end{pmatrix},$$

$$G(Y_1,Y_2)=\begin{pmatrix}[\beta(\eta_1E+I+\eta_2H)+\beta_1B]S-k_1E\\ (1-p)\kappa E-k_2A\\ p\kappa E-k_3I\\ \gamma_1A-k_4Q\\ \gamma_2I+\theta Q-k_5H\\ m_1A+m_2I-\sigma B\end{pmatrix}..$$

The disease-free equilibrium of system (1) is globally asymptotically stable if the two following conditions (H_1) and (H_2) are satisfied.

(H_1) For $\frac{dY_1}{dt}=F(Y_1,0),Y_1^0$ is globally asymptotically stable where $F(Y_1^0,0)=0.$

(H_2) $G(Y_1,0)=0$ and $G(Y_1,Y_2)=CY_2-\hat{G}(Y_1,Y_2),\hat{G}(Y_1,Y_2)\geq 0$ for $(Y_1,Y_2)\in\Omega$ and $C=D_{Y_2}G(Y_1^0,0)$ is a Metzler-matrix.

From the first equation of system (21),

$$\frac{dY_1}{dt}=F(Y_1,0)=\begin{pmatrix}\Lambda-\mu S\\ -\mu R\end{pmatrix}.\tag{22}$$

The solution of system (22) is

$$\begin{bmatrix}S(t)\\ R(t)\end{bmatrix}=\begin{bmatrix}\Lambda/\mu+(S^0-\Lambda/\mu)e^{-\mu t}\\ R^0e^{-\mu t}\end{bmatrix}.$$

It can be shown $S\to S^0=\Lambda/\mu$ and $R\to R^0=0$ as $t\to\infty$, indicating that the solution of (22) has global convergence. As a result, condition (H_1) is satisfied, and $Y_1^0=(S^0,R^0)$ is globally asymptotically stable.

Furthermore, we show that $G(Y_1,Y_2)$ satisfies the two conditions given in (H_2). It is clear that $G(Y_1,0)=0$. From the system (21), we obtain

$$C=D_{Y_2}G(Y_1^0,0)=\begin{pmatrix}-k_1 & \frac{\beta\eta_1\Lambda}{\mu} & \frac{\beta\Lambda}{\mu} & 0 & \frac{\beta\eta_2\Lambda}{\mu} & \frac{\beta_1\Lambda}{\mu}\\ (1-p)\kappa & -k_2 & 0 & 0 & 0 & 0\\ p\kappa & 0 & -k_3 & 0 & 0 & 0\\ 0 & \gamma_1 & 0 & -k_4 & 0 & 0\\ 0 & 0 & \gamma_2 & \theta & -k_5 & 0\\ 0 & m_1 & m_2 & 0 & 0 & -\sigma\end{pmatrix}.\tag{23}$$

and

$$\begin{aligned}\hat{G}(Y_1,Y_2)&=CZ-G(Y_1,Y_2)\\&=\begin{pmatrix}(S^0-S)[\beta(\eta_1A+I+\eta_2H)+\beta_1B]\\ 0\\ 0\\ 0\\ 0\\ 0\end{pmatrix}\end{aligned}\tag{24}$$

The matrix C is a Metzler-matrix because none of its off-diagonal entries are nonnegative. In the region Ω_1, $S\leq S^0$ and hence we have $S^0-S\geq 0$. The boundaries of the total population are $N\leq\Lambda/\mu$ and $B\leq m\Lambda/\sigma\mu$. We have $(S^0-S)[\beta(\eta_1A+I+\eta_2H)+\beta_1B]$ and $\hat{G}(Y_1,Y_2)\geq 0.$ As a result, $G(Y_1,Y_2)$ meets the two criteria, which suggests that condition (H_2) is met.

The proof of Theorem 1 is completed. □

E. Global Stability of Endemic Equilibrium

The Lyapunov asymptotic theorem is used to describe the global asymptotic stability of the endemic equilibrium. By referencing the research of Riyapan and Xu [31, 32], we will design a Lyapunov function from system (1).

Theorem 2 *If $\mathcal{R}_0>1$, then the endemic equilibrium X_1 of the system (1) is globally asymptotically stable in Ω.*

Proof. Let $\mathcal{R}_0>1$, such that the endemic equilibrium of system (1) X_1 exists. We consider the candidate Lyapunov function $\mathcal{L}$ as follows:

$$\begin{aligned}\mathcal{L}=\frac{1}{2}\Big[&\left(S-S^*\right)+\left(E-E^*\right)+\left(A-A^*\right)+\left(I-I^*\right)+\left(Q-Q^*\right)\\&+\left(H-H^*\right)+\left(R-R^*\right)\Big]^2+\frac{1}{2}\left(B-B^*\right)^2.\end{aligned}\tag{25}$$

The statement below gives the derivative of $\mathcal{L}$ along the solutions of system (1). The statement below gives the derivative along the solutions of system (1).

$$\begin{aligned}\frac{d\mathcal{L}}{dt}=\Big[&\left(S-S^*\right)+\left(E-E^*\right)+\left(A-A^*\right)+\left(I-I^*\right)+\left(Q-Q^*\right)\\&+\left(H-H^*\right)+\left(R-R^*\right)\Big]\frac{dN}{dt}+\left(B-B^*\right)\frac{dB}{dt}.\end{aligned}\tag{26}$$

From (6) and (7), all solutions of system (1) satisfy $N^*=\Lambda/\mu,\ B^*=m\Lambda/\sigma\mu,\ dN/dt\leq\Lambda-\mu N,\ dB/dt\leq m\Lambda/\mu-\sigma B.$ Thus, $d\mathcal{L}/dt\geq 0$ and

$$\begin{aligned}\frac{d\mathcal{L}}{dt}&=\Big[(S-S^*)+(E-E^*)+(A-A^*)+(I-I^*)+(Q-Q^*)\\&\quad+(H-H^*)+(R-R^*)\Big]\frac{dN}{dt}+(B-B^*)\frac{dB}{dt}\\&\leq(N-N^*)(\Lambda-\mu N)+(B-B^*)(\tfrac{m\Lambda}{\mu}-\sigma B)\\&=-\mu(N-\tfrac{\Lambda}{\mu})(N-\tfrac{\Lambda}{\mu})-\sigma(B-\tfrac{m\Lambda}{\sigma\mu})(B-\tfrac{m\Lambda}{\sigma\mu})\\&=-\mu(N-\tfrac{\Lambda}{\mu})^2-\sigma(B-\tfrac{m\Lambda}{\sigma\mu})^2\\&<0.\end{aligned}\tag{27}$$

Additionally, $d\mathcal{L}/dt = 0$ if and only if $N = \Lambda/\mu$ and $B = m\Lambda/\sigma\mu$ (or $S = S^*, E = E^*, A = A^*, I = I^*, Q = Q^*, H = H^*, R = R^*$, and $B = B^*$). Hence, $\mathcal{L}$ is a Lyapunov function on Ω. The biggest compact invariant set of system (1) in the set $\left\{(S,E,A,I,Q,H,R,B) \in \Omega : \frac{d\mathcal{L}}{dt} = 0\right\}$ is a singleton $\{X_1\}$. Then by LaSalle's Invariance Principle [23], the endemic equilibrium X_1 is globally asymptotically stable in Ω for $\mathcal{R}_0 > 1$.

The proof of Theorem 2 is completed. □

F. Sensitivity Analysis for $\mathcal{R}_0$

The effect of model parameter values on the output value of $\mathcal{R}_0$. Sensitivity analysis is used to measure how sensitive the basic reproduction number with respect to the model parameters. We perform the analysis by calculating the basic reproduction number is with respect to the model parameters.

We perform the analysis by calculating the sensitivity indices of $\mathcal{R}_0$ to the parameters in the model using the

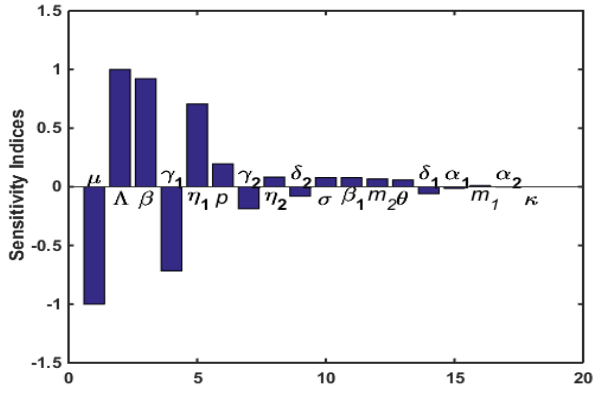

Fig. 2. Global sensitivity plot.

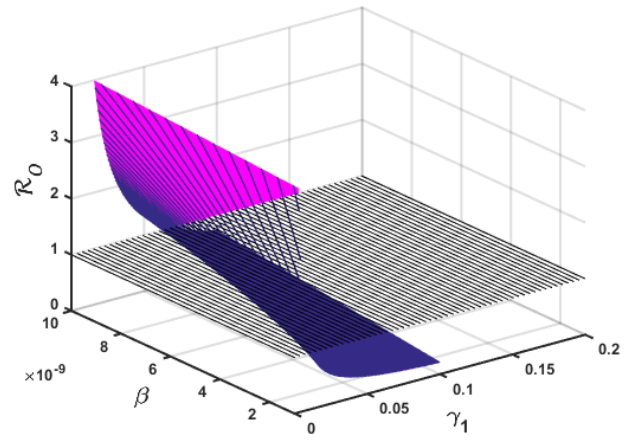

Fig. 3. The relationship among $\mathcal{R}_0$, β, and γ_1.

approach of [24]. The sensitivity index is used to measure the spread of the initial disease and the relative change in $\mathcal{R}_0$ if one parameter changes while other parameters remain. A sensitivity index on parameters with a high influence on $\mathcal{R}_0$ can be used to target intervention in order to control disease transmission. The sensitivity index can also be computed using partial derivatives when a variable is differentiable function of a model parameter.

TABLE III
SENSITIVITY INDEX OF $\mathcal{R}_0$ FOR MODEL PARAMETERS

Parameter	Sensitivity Index	Parameter	Sensitivity Index
μ	-1.0003	σ	+0.0782
Λ	+1.0000	β_1	+0.0782
β	+0.9218	m_2	+0.0673
γ_1	-0.7166	θ	+0.0593
η_1	+0.7058	δ_1	-0.0593
p	+0.1954	α_1	-0.0137
γ_2	-0.1870	m_1	+0.0109
η_2	+0.0825	α_2	-0.0025
δ_2	-0.0799	κ	+0.0002

Definition 1. *The normalized forward sensitivity index of a variable, $\mathcal{R}_0$, that depends differentiably on index on parameter, c is defined as*

$$\Upsilon_c^{\mathcal{R}_0} = \frac{\partial \mathcal{R}_0}{\partial c}\frac{c}{\mathcal{R}_0}. \tag{28}$$

Using parameter values from Table I, we calculate the sensitivity indices of $\mathcal{R}_0$ for all 18 parameters $(\mu, \Lambda, \beta, \gamma_1, \eta_1, p, \gamma_2, \eta_2, \delta_2, \sigma, \beta_1, m_2, \theta, \delta_1, \alpha_1, m_1, \alpha_2, \kappa)$ related to $\mathcal{R}_0$. We performed a sensitivity analysis using (28) with these parameters. The parameters are ordered from most sensitive to least sensitive. In practice, the natural death rate, disease death rate, and recruitment rate are not easy to control, so from Table III, it is concluded that the most sensitive parameter is β, followed by γ_1, and η_1. Fig. 2 depicts the sensitivity index values for all parameters in bar chart which corresponds to Table III.

In general, Table III indicates that by increasing one of the sensitivity indices with a positive sign $(\Lambda, \beta, \eta_1, p, \eta_2, \sigma, \beta_1, m_2, \theta, m_1, \kappa)$ while the other parameters constant, the value of $\mathcal{R}_0$ increases. This implies that they increase the endemicity of the disease. The value of $\mathcal{R}_0$ decreases when one of the sensitivity indices with a negative sign $(\mu, \gamma_1, \gamma_2, \delta_1, \delta_2, \alpha_1, \alpha_2)$ is increased while the other parameters remain constant. This means that they reduce the endemicity of the disease.

Table III shows that β represent the rate of transmission from the infected (A, I, H) to the susceptible and has a positive sensitivity index (+0.9218). This shows that an increase (or decrease) in β a by 10% will be followed by an increase (or decrease) in $\mathcal{R}_0$ by 9.218 %.

On the other hand, γ_1 represents the rate of quarantine and has a negative sensitivity index (-0.7166). This shows that a change of 10% in γ_1 will be immediately followed by a change of 7.166% in the basic reproduction number $\mathcal{R}_0$. The natural mortality rate (μ) and the recruitment rate of susceptibles (Λ), respectively, are linked to and the highest sensitivity index, respectively. We cannot utilize these factors as as control parameters since they are uncontrollable. The sensitivity index of the hospitalized rate

is -0.1870, which indicate that to reduce $\mathcal{R}_0$ we need to increase the hospitalized rate. The sensitivity index of recovery from hospitalized class (γ_2) is are -0.0799, which indicate that to reduce $\mathcal{R}_0$ we need to increase the recovery from hospitalized class. The sensitivity index of the natural decay rate of viruses from the environment surfaces (σ) is +0.0782, which indicates that to reduce $\mathcal{R}_0$ we need to decrease the natural decay rate of virus from the environment (surface). The sensitivity indices for γ_2 and σ are relatively small, which indicate that they have no effect on $\mathcal{R}_0$. The relationship between the basic reproduction number $\mathcal{R}_0$, the transmission rate β, and the quarantined rate γ_1 is depicted in Fig. 3. According to Fig. 3, even if γ_1 is large, the basic reproduction number $\mathcal{R}_0$ can be less than unit by decreasing the transmission rate β.

IV. Optimal Conttrol

A. The Formulation of Optimal Control Problem

Previously, we analyzed the impact of control interventions at a constant rate. In this section, we formulate the optimal control problem for COVID-19 by including five time-dependent controls in system (1). The first control variable is the awareness of wearing a medical mask, staying at home, and washing their hands to prevent the spread of COVID-19, as denoted by u_1. The control variable u_2 is a control variable used to improve hospitalized patient care in terms of intense medical treatment to increase the recover rate of hospitalized individuals. The control variable u_3 is surface disinfection, which is used to reduce the number of viruses on environmental surfaces. The controls are bounded between 0 and 1 in the intervention time interval [0, T], where T stands for the last time the controls were utilized. Thus, system (1) became

$$\begin{aligned}
\frac{dS}{dt} &= \Lambda - (1-u_1)[\beta(\eta_1 A + I + \eta_2 H) + \beta_1 B]S - \mu S,\\
\frac{dE}{dt} &= (1-u_1)[\beta(\eta_1 A + I + \eta_2 H) + \beta_1 B]S - (\kappa+\mu)E,\\
\frac{dA}{dt} &= (1-p)\kappa E - (\gamma_1+\mu)A,\\
\frac{dI}{dt} &= p\kappa E - (\gamma_2+\alpha_1+\mu)I,\\
\frac{dQ}{dt} &= \gamma_1 A - (\theta+\delta_1+\mu)Q,\\
\frac{dH}{dt} &= \gamma_2 I + \theta Q - (\delta_2+u_2+\alpha_2+\mu)H,\\
\frac{dR}{dt} &= \delta_1 Q + (\delta_2+u_2)H - \mu R,\\
\frac{dB}{dt} &= m_1 A + m_2 I - (\sigma+u_3)B.
\end{aligned} \tag{29}$$

Furthermore, it is also stated that there are bounds on the maximum rate of control measures in a given period.

B. Characterization of Optimal Control

Our goal is to minimize the number of infected humans (asymptomatic infected, symptomatic infected, hospitalized individuals), the pathogen population B (the concentration of coronavirus in the environmental reservoir), and the costs required to control COVID-19 by applying these five measures. The Pontryagin maximal principle [25] provides the necessary conditions for optimal control. According to PMP, the optimal control problem with the objective function is given by

$$J(u) = \int_0^T \left[b_1 A + b_2 I + b_3 H + b_4 B + \tfrac{1}{2}(c_1 u_1^2 + c_2 u_2^2 + c_3 u_3^2)\right] dt \tag{30}$$

where b_j, $j = 1, 2, 3, 4$ are the balance of the cost size of reducing the disease transmission and $c_i, i = 1, 2, 3$ are weights of the relative costs of the controls associated with the measures $u_1, u_2,$ and u_3 respectively. The goal is to create an optimal control, $u_1^2, u_2^2,$ and u_3^2 such that

$$J\left(u_1^*,\ u_2^*, u_3^*\right) \min_{u_i \in U} J\left(u_1(t), u_2(t), u_3(t)\right), \tag{31}$$

where the control set is given by $U = \left\{u_i(t) : 0 \le u_i(t) \le 1, i = 1, 2, 3,\ \forall t \in [0, T]\right\}$.

We will also use system (1) to determine the existence of an optimal control with the necessary conditions that satisfy Pontryagin's Maximum Principle [41]. The Pontryagin's Maximum Principle converts (1)-(3) into a problem of minimizing a pointwise Halmitonian function $\mathcal{H}$ with respect to u_i $(i = 1, 2, 3)$. The Lagrangian L for the above optimal control system is defined as

$$L = b_1 I_1 + b_2 I_2 + b_3 H + b_4 B + \tfrac{1}{2}(c_1 u_1^2 + c_2 u_2^2 + c_3 u_3^2) \tag{32}$$

The Hamiltonian function H is defined for all $t \in [0, T]$, as follows.

$$\begin{aligned}
\mathcal{H} &= b_1 A + b_2 I + b_3 H + b_4 B + \tfrac{1}{2}(c_1 u_1^2 + c_2 u_2^2 + c_3 u_3^2)\\
&+ \lambda_S\left(\Lambda - (1-u_1)[\beta(\eta_1 A + I + \eta_2 H) + \beta_1 B]S - \mu S\right)\\
&+ \lambda_E\left((1-u_1)[\beta(\eta_1 A + I + \eta_2 H) + \beta_1 B]S - (\kappa+\mu)E\right)\\
&+ \lambda_A\left((1-p)\kappa E - (\gamma_1+\mu)A\right)\\
&+ \lambda_I\left(p\kappa E - (\gamma_2+\alpha_1+\mu)I\right)\\
&+ \lambda_Q\left(\gamma_1 A - (\theta+\delta_1+\mu)Q\right)\\
&+ \lambda_H\left(\gamma_2 I + \theta Q - (\delta_2+u_2+\alpha_2+\mu)H\right)\\
&+ \lambda_R\left(\delta_1 Q + (\delta_2+u_2)H - \mu R\right)\\
&+ \lambda_B\left(m_1 A + m_2 I - (\sigma+u_3)B\right).
\end{aligned} \tag{33}$$

where $\lambda_S, \lambda_E, \lambda_A, \lambda_I, \lambda_Q, \lambda_H, \lambda_R,$ and λ_B are the adjoint variables.

Next, we examine the preconditions that must be met in order for a solution to the optimal control problem for system (1) to exist.

Theorem 3. *If $u^* = (u_1^*, u_2^*, u_3^*)$ is an optimal control and $\left(S^*, E^*, A^*, I^*, Q^*, H^*, R^*, B^*\right)$ are the solutions of the corresponding control system (1) that minimize the objective functional $J(u_1, u_2, u_3)$ over the control set U, then there exists an adjoint variable λ_j for $j = S, E, A, I, Q, H, R, B$,*

which satisfying

$$\begin{aligned}
\frac{d\lambda_S}{dt} &= (\lambda_S - \lambda_E)(1-u_1)[\beta(\eta_1 A + I + \eta_2 H) + \beta_1 B] + \lambda_S \mu,\\
\frac{d\lambda_E}{dt} &= (\lambda_E - \lambda_A)\kappa + (\lambda_A - \lambda_I)p\kappa + \lambda_E \mu,\\
\frac{d\lambda_A}{dt} &= -b_1 + (\lambda_S - \lambda_E)(1-u_1)\beta\eta_1 S + (\lambda_A - \lambda_Q)\gamma_1\\
&\quad + \lambda_A \mu - \lambda_B m_1,\\
\frac{d\lambda_I}{dt} &= -b_2 + (\lambda_S - \lambda_E)(1-u_1)\beta S + (\lambda_I - \lambda_H)\gamma_2\\
&\quad + \lambda_I(\alpha_1 + \mu) - \lambda_B m_2,\\
\frac{d\lambda_Q}{dt} &= (\lambda_Q - \lambda_H)\theta + (\lambda_Q - \lambda_R)\delta_1 + \lambda_Q \mu,\\
\frac{d\lambda_H}{dt} &= -b_3 + (\lambda_S - \lambda_E)(1-u_1)\beta\eta_2 S + (\lambda_H - \lambda_R)(\delta_2 + u_2)\\
&\quad + \lambda_H(\alpha_2 + \mu),\\
\frac{d\lambda_R}{dt} &= \lambda_R \mu,\\
\frac{d\lambda_B}{dt} &= -b_4 + (\lambda_S - \lambda_E)(1-u_1)\beta_1 S + \lambda_B(\sigma + u_3).
\end{aligned} \tag{34}$$

with transversality condition

$$\lambda_j(T) = 0 \text{ for } j = S, E, A, I, Q, H, R, B \tag{35}$$

Furthermore, the associated optimal controls u_1^*, u_2^*, and u_3^* are given by

$$\begin{aligned}
u_1^* &= \min\left\{1, \max\left\{0, \frac{(\lambda_E - \lambda_S)[\beta(\eta_1 A + I + \eta_2 H) + \beta_1 B]S}{c_1}\right\}\right\},\\
u_2^* &= \min\left\{1, \max\left\{0, \frac{(\lambda_H - \lambda_R)H}{c_2}\right\}\right\},\\
u_3^* &= \min\left\{1, \max\left\{0, \frac{\lambda_B B}{c_3}\right\}\right\}.
\end{aligned} \tag{36}$$

Proof. To determine whether optimal control exists, utilize the result from [26]. By differentiating the Hamiltonian function $\mathcal{H}$ in (33) with respect to the state variables *S*, *E*, *A*, *I*, *Q*, *H*, *R*, *W*, and *B*, we can obtain the adjoint equations (7.9) as follows:

$$\begin{aligned}
&\frac{d\lambda_S}{dt} = -\frac{d\mathcal{H}}{dS}, \quad \lambda_S(T) = 0; \quad \frac{d\lambda_E}{dt} = -\frac{d\mathcal{H}}{dE}, \quad \lambda_E(T) = 0;\\
&\frac{d\lambda_A}{dt} = -\frac{d\mathcal{H}}{dA}, \quad \lambda_{I_1}(T) = 0; \quad \frac{d\lambda_I}{dt} = -\frac{d\mathcal{H}}{dI}, \quad \lambda_I(T) = 0;\\
&\frac{d\lambda_Q}{dt} = -\frac{d\mathcal{H}}{dQ}, \quad \lambda_Q(T) = 0; \quad \frac{d\lambda_H}{dt} = -\frac{d\mathcal{H}}{dH}, \quad \lambda_H(T) = 0;\\
&\frac{d\lambda_R}{dt} = -\frac{d\mathcal{H}}{dR}, \quad \lambda_R(T) = 0; \quad \frac{d\lambda_B}{dt} = -\frac{d\mathcal{H}}{dB}, \quad \lambda_B(T) = 0.
\end{aligned} \tag{37}$$

Furthermore, to obtain the characterizations for the optimal control, we need to partially differentiate the Hamiltonian function $\mathcal{H}$ in (33) with respect to u_1, u_2, and u_3 on the control set *U*. The optimal control of system (1) is discovered using the following equations:

$$\begin{aligned}
\frac{\partial \mathcal{H}}{\partial u_1} &= c_1 u_1 + (\lambda_S - \lambda_E)[\beta(\eta_1 A + I + \eta_2 H) + \beta_1 B = 0\\
\frac{\partial \mathcal{H}}{\partial u_2} &= c_2 u_2 + (\lambda_R - \lambda_H)H = 0,\\
\frac{\partial \mathcal{H}}{\partial u_3} &= c_3 u_3 - \lambda_B B = 0.
\end{aligned} \tag{38}$$

Solving (38) for u_1, u_2, and u_3 gives

$$\begin{aligned}
\tilde{u}_1 &= \frac{(\lambda_E - \lambda_S)[\beta(\eta_1 A + I + \eta_2 H) + \beta_1 B]S}{c_1},\\
\tilde{u}_2 &= \frac{(\lambda_H - \lambda_R)H}{c_2},\\
\tilde{u}_3 &= \frac{\lambda_B B}{c_3}.
\end{aligned} \tag{39}$$

Finally, from common control arguments requiring bounds on the control, it follows that

$$u_i^* = \begin{cases} 0 & \text{if} \quad \tilde{u}_i < 0 \\ \tilde{u}_i & \text{if} \quad 0 \le \tilde{u}_i \le 1 \\ 1 & \text{if} \quad \tilde{u}_i > 1 \end{cases}, \tag{40}$$

where $i = 1, 2, 3$. As a result, the characterization in (36) can be derived.

The proof of Theorem 3 is completed. □

V. Numerical Simulation

A. Optimal Control Simulation

Using the parameter values in Table II, we can directly calculate the basic reproduction number $\mathcal{R}_0 = 1.433105$, indicating that the system has a globally asymptotically stable E_1 = (5.131228×10^6, 1466.7, 797.5, 95.3, 1651.1, 104.5, 8.9562×10^6, 327.4) equilibrium point. In this section, we perform only four numerical simulations of seven possible combinations of three intervention strategies (u_1, u_2, and u_3) to explore the most effective intervention strategies. With appropriate lower and upper bounds for the control and initial conditions for the state variables, the constraint system (29) and adjoint system (34) are solved forward in time and backward in time, respectively.

This simulation known as fourth-order Runge-Kutta forward-backward sweep simulation. For simulation purposes, we used the initial conditions *S*(0) = 30,416,000, *E*(0) = 15, *A*(0) = 15, *I*(0) = 12, *Q*(0) = 5, *H*(0) = 0, *R*(0) = 0, and *B*(0) = 0, together with the parameter values listed in Table I. The weight and cost associated with the objective function (5.2) are assumed to be $c_1 = 20, c_2 = 100, c_3 = 20$. The lower and upper bounds for the controls are assumed to be 0 and 1.

We consider and compare three control intervention schemes: a double control implementation and three control implementations combined. Thus, the simulations of optimal control are divided into four strategies: the use of a combination of u_1 and u_2 (Strategy A), the use of a control combination of u_1 and u_3 (Strategy B), the use of a

combination of u_2 and u_3 (Strategy C), and the use of a combination of u_1, u_2 and u_3 (Strategy D).

The following four scenarios were considered for numerical simulations:

Strategy A. The Use of a Combination of u_1 and u_2

Fig. 4 presents the numerical simulation with the implementation of the combination of two controls u_1 (the awareness about medical masks, staying at home, and hand washing) and u_2 (the intense medical treatment). Fig. 4 (a-b) demonstrates that the optimal control Strategy A can reduce the total number of infections averted ($A+I+H$) and the number of viruses on environmental surfaces (B) compared to not using the optimal control Strategy A. Figure 4 (c) depicts the control profile for this strategy. It can be seen that the usage of the awareness about medical mask, stay at home, and hand washing (u_1) measures needs to be optimally practiced (100%) for about the first 61 days and then gradually decrease to zero (lower bound). The usage of control u_2 (the intense medical treatment) was 0.16 at the start of the control period and then gradually decreased to the lower bound.

Strategy B. The Use of a Combination of u_1 and u_3

Fig. 5 shows the numerical simulation with the implementation of the combination of two controls, namely, the awareness about medical mask, stay at home, and hand washing (u_1) and the surface disinfection (u_3). According to Fig. 5(a-b), the use of Strategy B is the same as the simulation results by strategy A. The control profile for Strategy B is shown in Figure 5(c). It is observed that the controls u_1 and u_3 are kept 100% for the first 61 and 3 days of COVID-19 pandemic, respectively.

Strategy C. The Use of a Combination of u_2 and u_3

Fig. 6 presents the numerical simulation with the implementation of the combination of two controls u_2 (the intense medical treatment) and u_3 (the surface disinfection). Figs. 6(a) and 6(b) demonstrate that the optimal control Strategy A can reduced the total number of infections averted and the number of viruses on environmental surfaces (B) compared to not using the optimal control Strategy A. Figure 6(c) depicts the control profile for this strategy. It can be seen that the usage of awareness about medical masks, staying at home, and hand washing (u_1).

Strategy D. The Use of a Combination of u_1, u_2, and u_3

Fig. 7 shows the implementation of the combination of three controls: public health education or awareness about medical masks, staying at home, and hand washing (u_1), intense medical treatment (u_2), and surface disinfection (u_3). Figures 7(a-b) show that the total number of infections averted and the number of viruses on environmental surfaces removed by Strategy D are the same as the simulation results for strategy A or B. The control profile for Strategy D is shown in Figure 7 (c). It can be seen that the usage of this strategy should be maintained at optimally practiced levels for controls u_1 and u_3, respectively, at 61 and 3.3 days. After which, at the end of the control period, it progressively declined to zero. Comparatively, control u_2 was 0.15 at the start of the control period before gradually dropping to the lower bound.

TABLE II
PARAMETERS VALUES OF THE MODEL (1)

Parameter	Value (day^{-1})	References
Λ	271.23	[15]
β	6.038×10^{-8}	[18]
β_1	1.03×10^{-8}	[15]
μ	3.01×10^{-5}	[15]
η_1	0.6323	[18]
η_2	0.5642	[19]
p	0.0268	[19]
κ	0.1849	[19]
γ_1	0.3309	[19]
γ_2	0.0714	[19]
α_1	0.0048	[19]
α_2	0.0102	[19]
δ_1	0.1429	[19]
δ_2	0.3219	[19]
σ	0.3117	[18]
θ	0.0169	[18]
m_1	0.0178	[18]
m_2	0.9215	[18]

B. Cost-Effectiveness Analysis

In this session, cost-effectiveness analysis is used to evaluate and determine the most effective and cost-effective strategy from four competing strategies (A, B, C, and D). To examine the variations in health costs and results of alternative solutions for the same finite resources, we employ two methods of implementation: ICER, or incremental cost-effectiveness ratio and ACER, or average cost-effectiveness ratio.

The definitions of ICER for the two strategies *i* and *j* and ACER for strategy *k* are given as follows [19]:

$$\text{ICER} = \frac{\text{Difference in total costs of strategies } i \text{ and } j}{\text{Difference in total number of infectious averted of strategies } i \text{ and } j}. \quad (41)$$

$$\text{ICER} = \frac{\text{Total costs invested on the intervention}}{\text{Total number of infections averted using the intervention}}. \quad (42)$$

The numerator of ICER in (41) consists of the differences in intervention cost, cost of disease averted, and cost of prevented cases. While the ICER denominator in (41) evaluates the difference in health outcomes, including the total number of infectious diseases averted (the differences between infectious disease individuals without and with control measures), the total number of infectious diseases averted (TA) and viral loads eliminated (TV) with the strategy i used over a specified time period were calculated using the formula $TA(i) = \int_0^T (X - X^*)\, dt$ and $TV(i) = \int_0^T (B - B^*)\, dt$. Variable X is the number of the infectious individuals (A, I, H) without controls and X^* is the number of the infectious individuals (A^*, I^*, H^*) with

controls. B and B^* are the viral load on surfaces in the environment without and with controls, respectively.

Furthermore, the formula that defines the total cost (TC) for implementing optimal control for a strategy i is

$$TC(i) = \int_0^T \tfrac{1}{2}(c_1u_1^2 + c_2u_2^2 + c_3u_3^2)dt\,.$$

Table III shows the total number of infectious diseases averted, the total number of viruses on the surface, the total cost, and the objective values of the various strategies. This table shows the total number of infections averted after implementing different control strategies in ascending order, ordered in terms of the mean total number of diseases prevented and the total viral load removed.

TABLE III
TOTAL AVERTED, TOTAL VIRAL LOAD, TOTAL COST, AND J VALUE

Strategy	TA	TV	TC	J
C	1.072E+07	1.409E+07	4199.400	8.138E+07
A	8.764E+07	1.856E+07	635.1245	1413
B	8.764E+07	1.856E+07	747.7781	1231
D	8.764E+07	1.856E+07	752.1264	1231

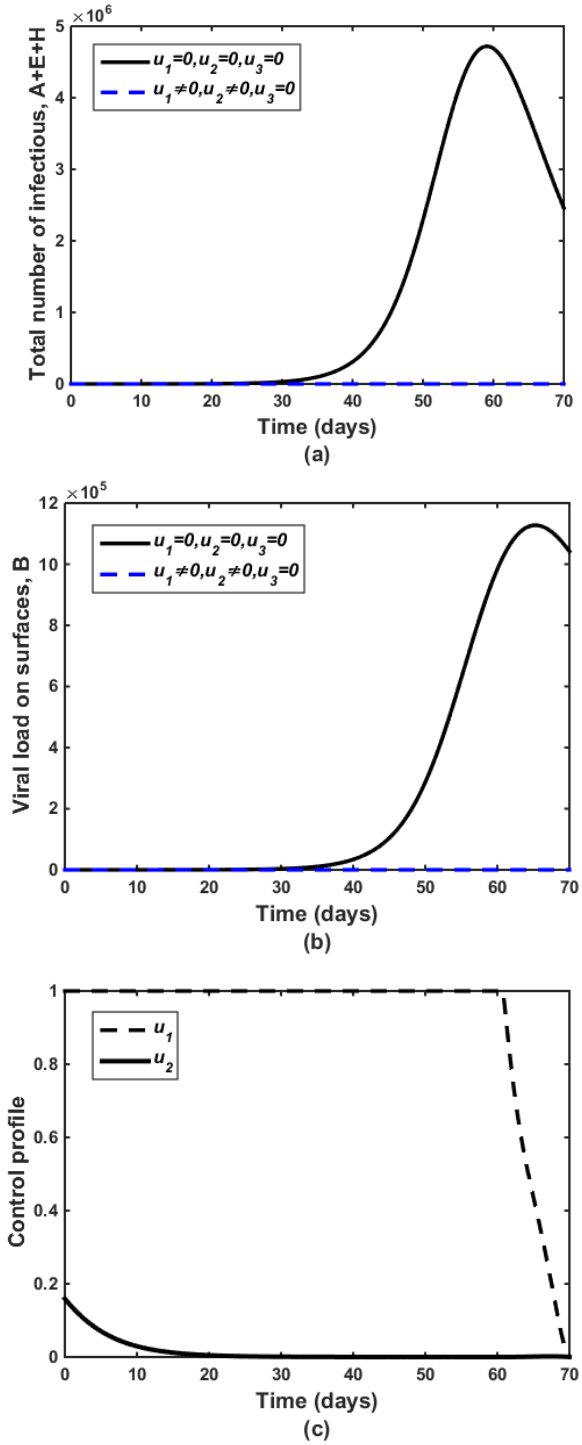

Fig. 4. Numerical simulation with the implementation of controls u_1 and u_2.

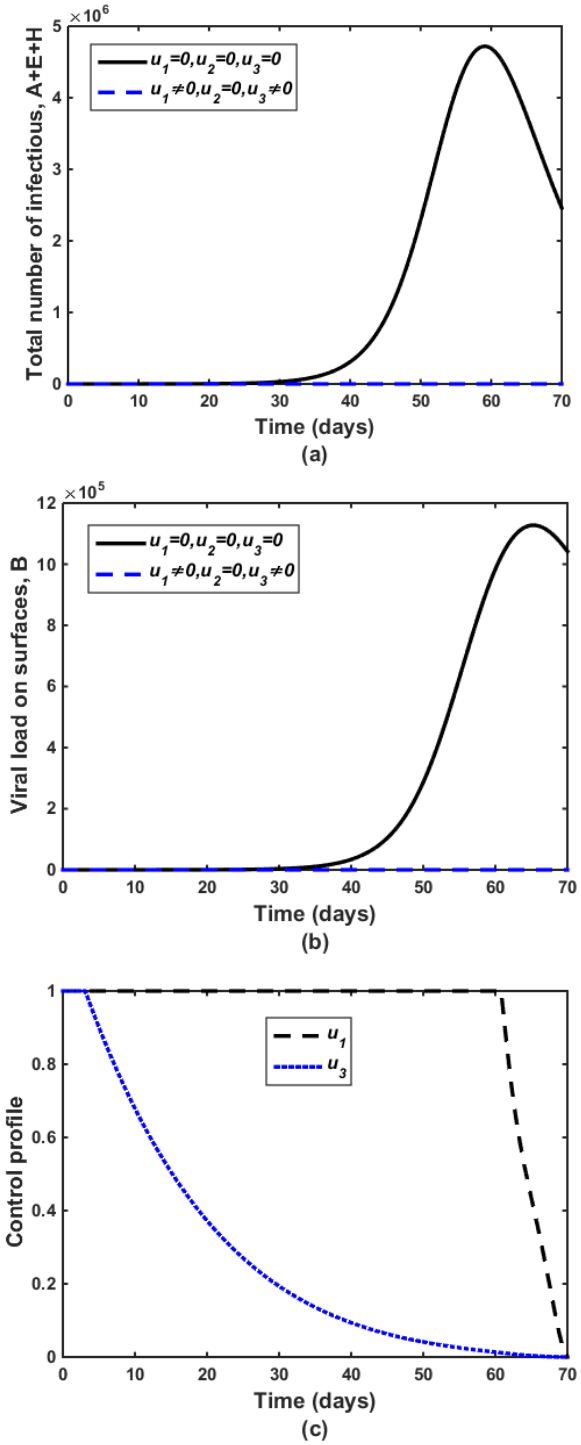

Fig. 5. Numerical simulation with the implementation of controls u_1 and u_3.

The overall number of infectious diseases avoided, the total number of viruses on the surface, the total cost, and the objective values of the various techniques are all displayed. The lowest cost value is associated with the control implementation utilizing strategy C, which is followed by strategy A in Table III. On the other hand, the control application using strategy D (or B) has the highest cost value and the lowest objective value.

To incrementally compare the two competing strategies, the ICER for strategies C and A is calculated using the ICER formula (41) as follows:

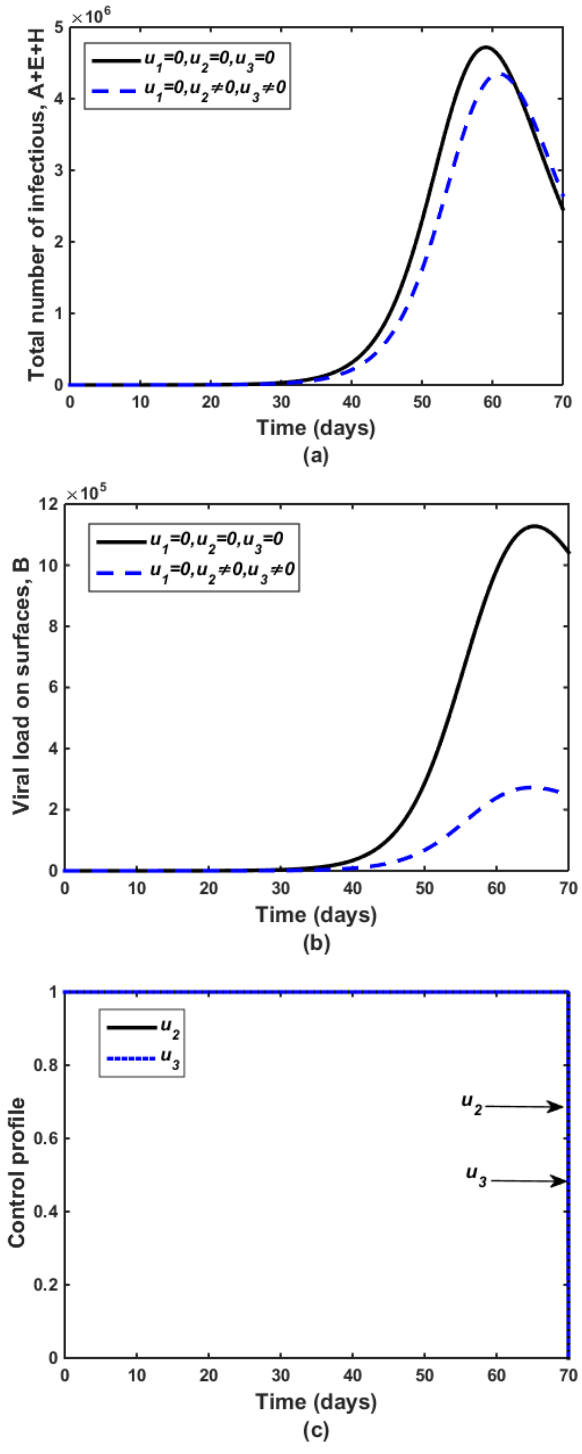

Fig. 6. Numerical simulation with the implementation of controls u_2 and u_3.

TABLE IV
COMPARISON OF STRATEGIES C AND A FOR INTERVENTION CONTROLS

Strategy	TA	TC	ACER	ICER
C	1.072e+07	4199.400	3,92E-07	3.92E+04
A	8.764e+07	635.1245	7,25E-06	-4.63E-05
B	8.764e+07	747.7781	8,53E-06	-
D	8.764e+07	752.1264	8,53E-06	-

$$\text{ICER(C)} = \frac{4.199\text{E}+03}{1,072\text{E}+07} = 3.92\text{E}+04,$$

$$\text{ICER(A)} = \frac{635.1245 - 4199.4}{8.764\text{E}+07 - 1.072\text{E}+07} = -4.63\text{E}-05.$$

From Table IV, it can be seen that ICER (C) has a higher value than ICER (A). This means that using the combination of two controls u_2 (the intense medical treatment) and u_3 (the surface disinfection). Thus, strategy C is excluded from the list of potential control interventions competing for the same limited resources, and then we compare control intervention strategies A and B using a similar procedure, as shown in Table V.

Note that, because the total number of infections averted by the three competing strategies A, B, and D is the same, the ICER for those methods does not need to be

TABLE V
COMPARISON OF STRATEGIES A, B, AND D FOR INTERVENTION CONTROLS

Strategy	TA	TC	ICER	ICER
A	8.764e+07	635.1245	7,25E-06	7.247E-06
B	8.764e+07	747.7781	8,53E-06	-
D	8.764e+07	752.1264	8,58E-06	-

recalculated. This cost analysis method states that the most cost-effective option is the one with the lowest ACER value. Table V shows that implementing Strategy A is the most economically advantageous option, followed by Strategy B and lastly Strategy D. The outcome is inconsistent with strategy B's (or D's) objective function value, which is the lowest of the four strategies.

Therefore, in this study, strategy A, which combines of two controls u_1 (awareness about medical masks, staying at home, and hand washing) and u_2 (the intense medical treatment), is considered to be the most economically sound option. From numerical simulation and the cost-effectiveness analysis for the four optimum control strategies, it was discovered that when the four control strategies were compared. In the absence of immunization, Strategy A (using physical or social distancing protocols) was the most cost-effective and effective control intervention. However, we observe that techniques A, B, and D are similarly effective at containing COVID-19 in terms of infection prevention.

VI. CONCLUSION

In this study, we create and examine a mathematical model of COVID-19 transmission that incorporates public health education (awareness about medical masks, staying at home, and hand washing), intense medical treatment, and surface disinfection interventions is created and examined.

In the first part, we perform a theoretical analysis of the model, including proving the positivity and boundedness of the solution using differential equation theory, establishing two equilibrium points (disease-free and endemic), determining the basic reproduction number expression via the generation matrix approach, demonstrating the disease-free equilibrium point and endemic equilibrium point are global stable by building the Lyapunov function, and using the Lasalle invariant principle. Then the model was developed by adding three control variables: public health education (u_1), intense medical treatment (u_2), and surface disinfectant (u_3). Three control expressions are produced using Pontryagin's maximal principle,

In the second part, we run numerical simulations. Through sensitivity analysis, the sensitivity index for each parameter to the basic reproduction number is obtained. Next, employing the fourth-order Runge-Kutta numerical scheme and the forward-backwards sweep method. We tried out the four different strategies and checked what happened and obtained the four optimal strategies, which were visually demonstrated in the form of plots of total infected cases, virus on the surface, and control profiles for each strategy. The four optimal strategies were then analyzed using average cost-effectiveness ratio (ACER) and cost-effectiveness analysis (ICER), yielding three final strategies, namely, Strategy A (a combination of the public health education and the intense medical treatment), Strategy B (a combination of the public health education and the surface disinfectant), and Strategy D (a combination of three controls) with the same number of averted infections. As a result, the total cost value and the objective function value of the strategy are utilized to determine which is most effective, with strategy A being the most effective. However, we found that, in terms of preventing infection, Strategies A, B, and D were similarly successful in containing COVID-19.

This study suggests that future research should consider extending the model to account for the impact of vaccination on reducing the number of COVID-19 cases and develop strategies that are cost-effective and low-impact. Further studies using appropriate factual data sets are encouraged to have a better understanding of the dynamics of disease transmission.

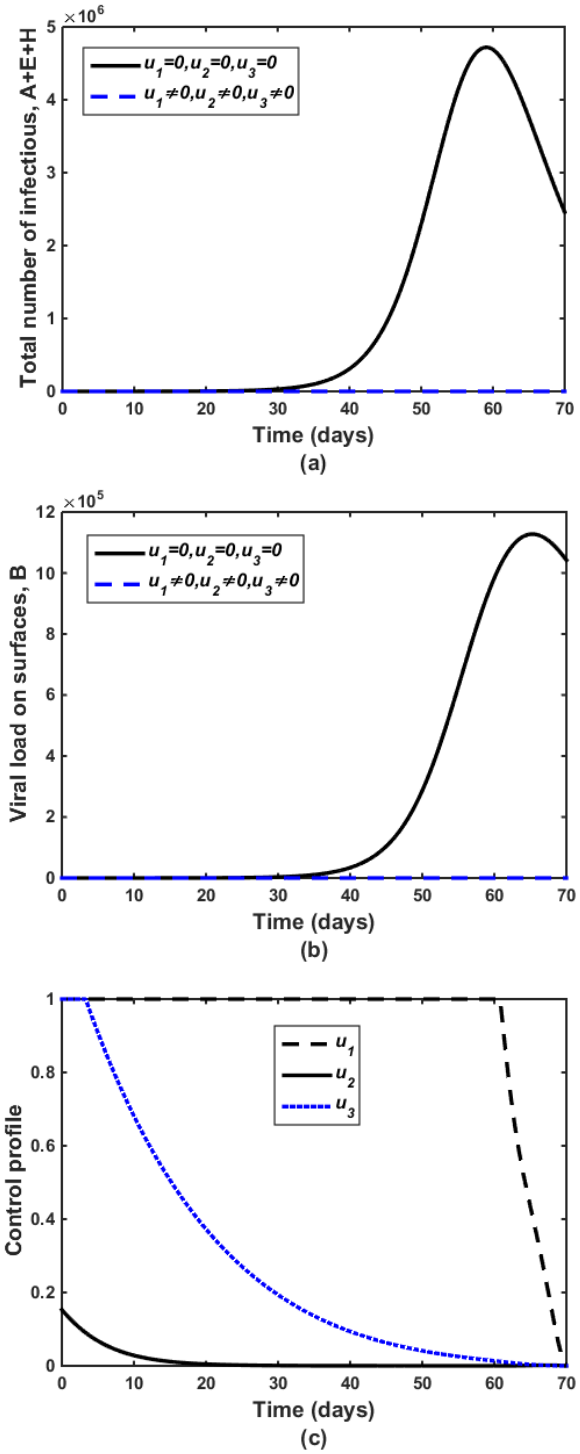

Fig. 7. Numerical simulation with the implementation for all controls u_1, u_2, dan u_3.

REFERENCES

[1] World Health Organization, "*Coronavirus Disease (COVID-19) Outbreak Situation*," Retrieved from https://www.who.int/emergencies/diseases/novel-coronavirus-2019 on 20th September 2022.

[2] I. Ahmed, G. U. Modu,, A. Yusuf, P. Kumam, and I. Yusuf, " A Mathematical Model of Coronavirus Disease (COVID-19) Containing Asymptomatic and Symptomatic Classes," *Results in Physics*, vol. 21, 103776, 2021.

[3] A. E. Gorbalenya, S. C. Baker, R. S. Baric , R. J. de Groot, C. Drosten, A. A. Gulyaeva1 et al., "Severe acuterespiratory syndrome-related coronavirus-The species and its viruses, a statement of the Coronavirus Study Group," *bioRxiv* (preprint), pp. 1-15, 2020.

[4] C. N. Ngonghala, E. Iboi, S. Eikenberry, M. Scotch, C. R. Macintyre, M. H. Bonds, A. M. Gumel, "Mathematical assessment of the impact of non-pharmaceutical interventions on curtailing the 2019 novel coronavirus," *Math. Biosci*., vol. 325, Article ID 108364, 2020 .

[5] S. A. Iyaniwura, M. Rabiu, J. F. David, J.D. Kong, "Assessing the impact of adherence to Non-pharmaceutical interventions and indirect transmission on the dynamics of COVID-19: a mathematical modelling study," *Mathematical Biosciences and Engineering*, vol. 18, no. 6, pp. 8905-8932, 2021.

[6] A. Perkins and G. Espana, "Optimal control of the COVID-19 pandemic with non-pharmaceutical interventions," *Bull Math Biol*, vol. 82, no. 9, Article ID 118, 2020.

[7] G. Kampf, D. Todt, S. Pfaender, and E. V. Steinmann, "Existence of coronaviruses on inanimate surfaces and their inactivation with biocidal agents, *Journal of Hospital Infection*, vol. 104, no. 3, pp. 8905-8932, 2020.

[8] S. Ullah and M. A. Khan, "Modeling the impact of non-pharmaceutical interventions on the dynamics of novel coronavirus with optimal control analysis with a case study," *Chaos, Solitons & Fractals*, vol. 139, Article ID 110075, 2020.

[9] N. Piovella, "Analytical solution of SEIR model describing the free spread of the COVID-19 pandemic," *Chaos, Solitons & Fractals*, vol. 140, Article ID 110243, 2020.

[10] S. Rezapour, H. Mohammadi and M. E. Samei, "SEIR epidemic model for covid-19 transmission by caputo derivative of fractional

order," *Advances in difference equations*, vol. 2020, no. 1, Article ID 490, 2020.
[11] S. Annas, M. I. Pratama, M. Rifandi, W. Sanusi, and S. Side, "Stability analysis and numerical simulation of SEIR model for pandemic COVID-19 spread in Indonesia," *Chaos, Solitons & Fractals*, vol. 139, Article ID 110072, 2020.
[12] H. M. Youssef, N. A. Alghamdi, M. A. Ezzat, A. A. El-Bary, and A. M. Shawky, "A new dynamical modeling SEIR with global analysis applied to the real data of spreading COVID-19 in Saudi Arabia," *Biosciences and Engineering*, vol. 17, no. 6, pp. 7018-7044, 2020.
[13] H. Zhao, N. N. Merchant, A. McNulty et al., "COVID-19: Short term prediction model using daily incidence data," *PLoS ONE*, vol. 16, no. 4, Article ID e0250110, 2021.
[14] N. Anggriani, M. Z. Ndii, R. Amelia, W. Suryaningrat, and M. A. A. Pratama, "A mathematical COVID-19 model considering asymptomatic and symptomatic classes with waning immunity," *Alexandria Eng J*, vol. 61, no.1, pp. 113–124, 2022.
[15] L. L. Obsu and S. F. Balcha, "Optimal control strategies for the transmission risk of COVID-19," *Journal of Biological Dynamics*, vol. 14, no. 1, pp. 590–607, 2020.
[16] D. Aldila, S. A. Khoshnaw, E. Safitri et al.," A mathematical study on the spread of COVID-19 considering social distancing and rapid assessment: The case of Jakarta, Indonesia," *Chaos, Solitons & Fractals*, vol. 139, Article ID 110042, 2020.
[17] X-F Luo, J-Y Yang, S. Feng, X-L Peng, X. Cao, J, Zheng et al.," Nonpharmaceutical intervention contribute to the control of COVID-19 in China based on a pairwise model," *Infections Disease Modeling*, vol. 6, pp. 643-663, 2021.
[18] J. K. K. Asamoah, M. A. Owusu, Z. Jin et al.," Global stability and cost-effectiveness analysis of COVID-19 considering the impact of the environment: using data from Ghana," *Chaos, Solitons & Fractals*, vol. 140, Article ID 110103, 2020.
[19] J. K. K. Asamoah, Z. Jin, G-Q. Sun et al.," Sensitivity assessment and optimal economic evaluation of a new COVID-19 compartmental epidemic model with control interventions," *Chaos, Solitons & Fractals*, vol. 1406, Article ID 110885, 2021.
[20] V. Lakshmikantham, S. Leela, A. and A. Martynyuk, "*Stability Analysis of Nonlinear Systems*, Marcel Dekker, Inc., New York and Basel, 1989.
[21] Van den Driessche and J. Watmough," Reproduction numbers and subthreshold endemic equilibria for compartmental models of disease transmission," *Mathematical Biosciences*, vol. 180, no. 1-2, pp. 29–48, 2002.
[22] C. Castillo-Chavez, Z. Feng, and W. Huang, "*On the Computation of R_o and Its Role on Global Stability*, *Mathematical Approaches for Emerging and Reemerging Infectious Diseases: An Introduction*," New York: IMA, Springer, 2002.
[23] J. P. La Salle, The Stability of Dynamical Systems, In: CBMS-NSF Regional Conference Series in Applied Mathematics," Philadelphia: Pa: SIAM,, 1976.
[24] N. Chitnis, J. M. Hyman, and J. M. Cushing, "Determining Important Parameter in the Spread of Malaria Through the Sensitivity Analysis of Mathematical Model," *Bulletin of Mathematical Biology*, vol. 70, no. 5, pp. 1272-1296, 2008.
[25] L.S. Pontryagin, V.G. Boltyanskii, R.V. Gamkrelidze, E.F. Mishchenko," *The Mathematical Theory of Optimal Processes*," New York: Wiley, 1962.
[26] W. H. Fleming, R. W. Rishel," *Deterministic and stochastic Optimal Control*," New York: Springer, 1975.
[27] F. B. Agusto and I. M. Elmojtaba, "Optimal control and cost-effective analysis of malaria/visceral leishmaniasis co-infection," *PLoS ONE* , vol. 12, no. 2, Article ID e0171102, 2017.
[28] Marsudi, Trisilowati, A. Suryanto, and I. Darti," Global Stability and Optimal Control of an HIV/AIDS Epidemic Model with Behavioral Change and Treatmen," *Engineering Letters*, vol. 29, no. 2, pp. 575-591, 2021.
[29] S. Olaniyi, O. Obabiyi, K. Okosun, A. Oladipo, and S. Adewale," Mathematical modelling and optimal cost-effective control of COVID-19 transmission dynamics," *European Physical Journal Plus*, vol. 135, no. 11, pp. 1-20, 2020.
[30] J. K. K. Asamoah, E. Okyere, A. Abidemi et al.," Optimal control and comprehensive cost-effectiveness analysis for COVID-19," *Appl Math Model*, vol. 90, pp. 719–741, 2022.
[31] D. G. Xu, X. Y. Xu, C. H. Yang, and W. H. Gui, "Global stability of a variation epidemic spreading model on complex nettworks," Mathematical Problems in Engineering, vol. 2015, Article ID 365049, 2015.
[32] P. Riyapan, S. E. Shuaib, and A. Intarasit, "A Mathematical Model of COVID-19 Pandemic: A Case Study of Bangkok, Thailand,"*Computational and Mathematical Methods in Medicine*, vol. 2021, Article ID 6664483, 2021.

Marsudi (M'19). Marsudi was born on January 17, 1961 in Magetan, East Java, Indonesia. In 1987, Marsudi graduated from Universitas Gadjah Mada (UGM), Yogyakarta, Indonesia with a bachelor of mathematics. In 1992, Marsudi received a Master of Science in Mathematics from Institut Teknologi Bandung (ITB). Marsudi graduated with a Doctoral in Applied Mathematics (Biology Mathematics) from Universitas Brawijaya (UB) in 2021.

He has more than 35 years of teaching experience in the Mathematics Department, Faculty of Mathematics and Natural Sciences, Universitas Brawijaya, Malang, Indonesia. Numerous research funds have been given out by Indonesia's Minister of Research and Technology for Higher Education. Current and previous research subjects in the disciplines of applied mathematics and mathematical modeling include epidemic modeling of infectious illnesses, optimization, and optimum control.

Other than the IAENG, Dr. Marsudi belongs to the IndoMS (Indonesian Mathematical Society). The Indonesian Biomathematical Society (IBMS) and the biomathematical research team at Universitas Brawijaya are currently under his direction.

Nur Shofianah. Nur Shofianah was born in Gresik, Indonesia on November 24, 1984. In 2007, Nur Shofianah graduated from Institut Teknologi Sepuluh Nopember Surabaya (ITS), Surabaya, Indonesia with a bachelor of mathematics. In 2009, Nur Shofianah received a Master of Science in Mathematics from the same institution. In 2014, Kanazawa University in Japan awarded Nur Shofianah a Ph.D in computational mathematics.

In the Mathematics Department of the Faculty of Mathematics and Natural Sciences at Universitas Brawijaya in Malang, Indonesia, she has more than 14 years of teaching experience. She actively takes part in conferences, workshops, and seminars related to science. There have been several research grants awarded by Indonesia's Minister of Research and Technology, Higher Education. Applied mathematics, mathematical modeling, and control theory are some of my current and past research interests.

Nur Shofianah, Ph.D is currently in charge of the Indonesian Biomathematical Society (IBMS) and the Biomathematical Research Group at UB.

Ummu Habibah. Ummu Habibah was born in Surabaya, Indonesia on May 15, 1985. In 2007, Ummu Habibah graduated from Institut Teknologi Sepuluh Nopember Surabaya (ITS), Surabaya, Indonesia with a bachelor of mathematics. In 2009, Ummu Habibah received a Master of Science in Mathematics from the same institution. At Kyushu University in Japan, Ummu Habibah earned her Ph.D. in mathematics in 2016.

In the Mathematics Department of the Faculty of Mathematics and Natural Sciences at Universitas Brawijaya in Malang, Indonesia, she has more than 14 years of teaching experience. She actively takes part in conferences, workshops, and seminars related to science. There have been several research grants awarded by Indonesia's Minister of Research and Technology, Higher Education. Applied mathematics, mathematical modeling, and control theory are some of my current and past research interests.

Ummu Habibah, PhD is currently in charge of the Indonesian Biomathematical Society (IBMS) and the Biomathematical Research Group at UB.